

---

# MLGIB: Multi-Label Graph Information Bottleneck for Expressive and Robust Message Passing

---

Chaokai Wu, Haofu Shi, Ningxuan Ma, Jianghong Ma, Xiaofeng Zhang

## Abstract

Graph Neural Networks (GNNs) suffer from over-squashing in deep message passing, where information from exponentially growing neighborhoods is compressed into fixed-dimensional representations. We show that this issue becomes a distinct failure mode in multi-label graphs: neighboring nodes often share only limited labels while differing across many irrelevant ones, causing predictive signals to be diluted by noisy label information. To address this challenge, we propose the *Multi-Label Graph Information Bottleneck* (MLGIB), which formulates multi-label message passing as constrained information transmission under irrelevant label noise. MLGIB balances expressiveness and robustness by preserving predictive label signals while suppressing irrelevant noise. Specifically, it constructs a Markovian dependence space and derives tractable variational bounds, where the lower bound maximizes mutual information with target labels and the upper bound constrains redundant source information. These bounds lead to an end-to-end label-aware message-passing architecture. Extensive experiments on multiple benchmarks demonstrate consistent improvements over existing methods, validating the effectiveness and generality of the proposed framework.

## 1 Introduction

Graph Neural Networks (GNNs) are widely used for modeling structured data [1–5], but deeper message passing often suffers from over-squashing, where information from exponentially growing neighborhoods is compressed into fixed-dimensional embeddings, causing the loss of long-range dependencies [6, 7]. While this issue has been studied mainly in homophilous graphs [8, 9], we show that it induces a distinct failure mode in multi-label graphs.

Unlike conventional homophilous graphs [10–12] under the single-label setting, where neighboring nodes are typically assumed to share the same class label, multi-label graphs [13–17] present a more intricate propagation scenario. As illustrated in Fig. 1(a), nodes in multi-label graphs typically share only a few labels while differing across many irrelevant ones. Additional statistics in Appendix Fig. 7 further support this observation. Thus, message passing [18, 19] expands the receptive field but also introduces increasingly noisy, partially relevant label signals, making aggregation ambiguous and effectively turning message passing into a noisy channel [6, 20, 21]. As shown in Fig. 1(b), after  $l$  layers of message passing, a target node  $v$  is inundated with mixed signals from its multi-hop neighborhood, where a small fraction of label information may be relevant while a large portion corresponds to irrelevant labels. Such noisy accumulation can quickly saturate node representations before meaningful long-range dependencies are effectively integrated. This indicates that over-squashing is not merely caused by structural compression, but also by the limited ability of GNNs to extract *informative signals from partially overlapping label information*.

This observation exposes two limitations of existing methods, as shown in Fig. 1(c). (1) Existing multi-label graph learning methods [22–24] model label correlations, but *lack sufficient expressiveness to preserve informative label signals* when they are entangled with irrelevant ones during multi-label propagation, causing predictive information to be diluted by irrelevant labels. (2) Current over-

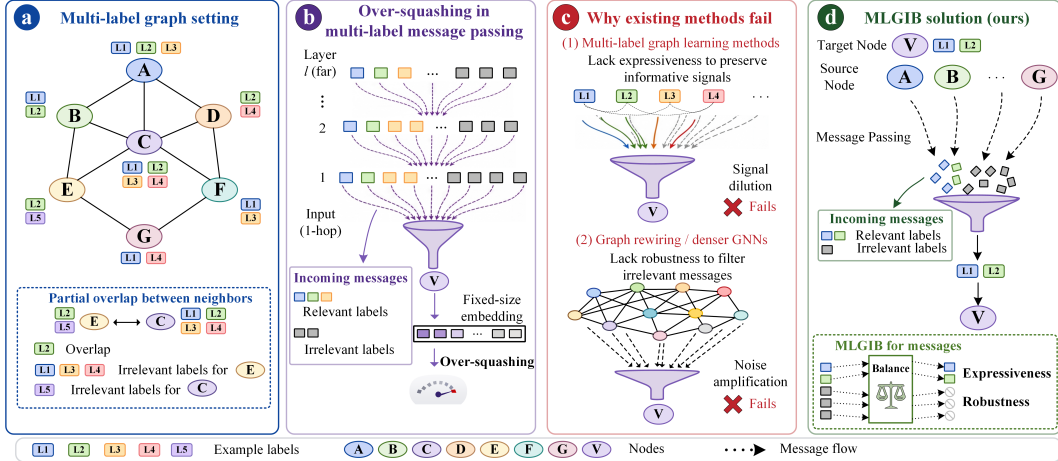


Figure 1: (a) The partial overlap problem of labels in multi-label graphs; (b) The manifestation of over-squashing in multi-label graphs, where exponentially growing label information is compressed into a fixed-dimensional vector; (c) Existing methods either struggle to extract truly informative label signals or introduce additional noise; (d) MLGIB can extract useful label information while reducing interference from irrelevant noise, exhibiting excellent expressiveness and robustness.

squashing mitigation methods, such as graph rewiring [25, 26, 7], improve structural connectivity but *lack robustness to filter irrelevant messages*, thereby amplifying noise in multi-label graphs. Together, these limitations suggest that effective multi-label message passing requires both expressiveness to preserve predictive label signals and robustness to suppress irrelevant noise.

To address the above limitations, we formulate multi-label message passing as an information-theoretic problem of transmitting predictive label signals under irrelevant noise. As shown in Fig. 1(d), we propose the Multi-Label Graph Information Bottleneck (MLGIB), which balances two complementary objectives: *expressiveness*, which preserves predictive label information during propagation, and *robustness*, which suppresses noise from irrelevant labels. To realize this principle, MLGIB constructs a Markovian dependence space tailored to multi-label graphs and optimizes it via tractable variational bounds. The upper bound limits redundant information induced by irrelevant labels, while the lower bound maximizes the mutual information of relevant predictive label signals. These bounds guide the design of an end-to-end differentiable message-passing architecture.

- To the best of our knowledge, this is the *first* work to extend the Information Bottleneck principle to multi-label graph learning, revealing that partial label overlap exacerbates over-squashing during message passing and motivates principled information filtering.
- We propose the Multi-Label Graph Information Bottleneck (MLGIB), a principled framework that formulates multi-label message passing as a constrained information transmission problem, enhancing the expressiveness and robustness in message passing.
- We instantiate MLGIB into a practical message-passing architecture tailored to multi-label graphs, incorporating label-aware information filtering into the propagation process.
- We conduct extensive experiments on multiple benchmark datasets, demonstrating consistent improvements over existing methods across different evaluation settings.

## 2 Preliminaries and Notations

### 2.1 Information Bottleneck in Deep Networks

Given input data  $X$  and target variable  $Y$ , deep networks aim to learn an intermediate representation  $Z_X$  that is maximally informative for predicting  $Y$ .  $Z_X$  is generated by a parametric encoder  $p(z|x)$ , where  $x$  and  $z$  denote instances of  $X$  and  $Z_X$ , respectively. The predictive information in  $Z_X$  can be measured by the mutual information between  $Z_X$  and  $Y$ :

$$I(Z_X; Y) = \int dz dy p(z, y) \log \frac{p(z, y)}{p(z)p(y)}, \quad (1)$$

where  $y$  is an instance of  $Y$ . However, directly maximizing  $I(Z_X; Y)$  may lead to a trivial solution, e.g., setting  $Z_X = X$ , which preserves all input information but does not yield a compact representation. The Information Bottleneck (IB) principle [27–29] addresses this by constraining the information  $Z_X$  retains about the input  $X$ . Specifically, it imposes the constraint  $I(Z_X; X) \leq I_c$ , where  $I_c$  denotes the information budget, leading to the constrained optimization problem:

$$\max I(Z_X; Y) \text{ s.t. } I(X; Z_X) \leq I_c. \quad (2)$$

By introducing a Lagrange multiplier  $\beta$ , the objective can be equivalently written as

$$\min \text{IB}(Z_X, Y, X) \triangleq -I(Z_X; Y) + \beta I(X; Z_X). \quad (3)$$

This objective encourages  $Z_X$  to preserve task-relevant information about  $Y$  while discarding redundant or irrelevant information from  $X$ .

## 2.2 Graph Information Bottleneck

The Graph Information Bottleneck (GIB) [30] principle extends IB to graph-structured data. Given graph data  $\mathcal{D}$  and prediction target  $Y$ , GIB aims to learn node representations  $Z_X$  that maximize predictive information about  $Y$  while minimizing redundant information from the original graph  $\mathcal{D}$ . To approximate the optimal representation, GIB defines a Markovian dependence space  $\Omega$  over the message-passing process. The GIB objective is formulated as

$$\min_{\mathbb{P}(Z_X^{(L)} | \mathcal{D}) \in \Omega} \text{GIB}(\mathcal{D}, Y; Z_X^{(L)}) \triangleq \left[ -I(Y; Z_X^{(L)}) + \beta I(\mathcal{D}; Z_X^{(L)}) \right]. \quad (4)$$

In this formulation, GIB purifies node representations by optimizing the mutual information  $I(Y; Z_X^{(L)})$  and  $I(\mathcal{D}; Z_X^{(L)})$ , making  $Z_X^{(L)}$  more predictive of  $Y$  while being less dependent on redundant graph information. However, under multi-label settings, the central challenge is no longer merely to purify node representations from graph-structured redundancy. Instead, it is to selectively preserve informative label signals from source nodes while suppressing irrelevant label noise during message propagation. This motivates Multi-Label Graph Information Bottleneck, which models multi-label message passing as a constrained information transmission problem.

## 3 Multi-Label Graph Information Bottleneck

### 3.1 Deriving the Multi-Label Graph Information Bottleneck

We introduce the Multi-Label Graph Information Bottleneck (MLGIB) to formulate multi-label message passing as a constrained information transmission problem. Given source-node data  $\mathcal{D}_s = (A, X)$ , where  $A$  denotes the graph structure from the source, MLGIB aims to learn messages  $Z_H$  that preserve predictive information about the target-node labels  $Y_t$  while suppressing redundant information from  $\mathcal{D}_s$ . To optimize this principle, we follow the local-dependence assumption in GIB [30], which states that, conditioned on nodes within a  $l$ -hop neighborhood of  $v$ , the remaining graph data is independent of  $v$ . Based on this assumption, we construct a Markovian dependence space  $\mathcal{M}$  for multi-label message passing:

$$\mathcal{M} = \begin{cases} A, Z_X^{(l)} \rightarrow Z_A^{(l)} \\ Z_A^{(l)}, Z_X^{(l)} \rightarrow Z_H^{(l)} \\ Z_H^{(l)}, Z_A^{(l)} \rightarrow Z_X^{(l+1)} \end{cases}, \quad (5)$$

where  $Z_X^{(0)} = X$ , and  $0 \leq l \leq L$  denotes the message-passing layer. This dependence space characterizes the generation process of  $\mathbb{P}(Z_X^{(l+1)} | \mathcal{D}_s)$ . Starting from the source-node data  $\mathcal{D}_s$ , each layer first refines the message-passing structure  $Z_A^{(l)}$ , then extracts messages  $Z_H^{(l)}$ , and finally updates the node representation  $Z_X^{(l+1)}$ . The key distinction of MLGIB lies in optimizing  $\mathbb{P}(Z_H^{(l)} | \mathcal{D}_s)$ , which can be decomposed into  $\mathbb{P}(Z_A^{(l)} | \mathcal{D}_s)$  and  $\mathbb{P}(Z_H^{(l)} | Z_A^{(l)}, Z_X^{(l)})$ . The former controls the message-passing paths, while the latter regulates message purity by selecting informative label signals and suppressing irrelevant noise. Following the intuition in Fig. 1, we define the MLGIB objective as

$$\min_{\mathbb{P}(Z_H^{(L)} | \mathcal{D}_s) \in \mathcal{M}} \text{MLGIB}(\mathcal{D}_s, Y_t; Z_H^{(L)}) \triangleq \left[ -I(Y_t; Z_H^{(L)}) + \beta I(\mathcal{D}_s; Z_H^{(L)}) \right]. \quad (6)$$

The first term encourages *expressiveness* by maximizing the predictive information between the learned messages and target-node labels, while the second term promotes *robustness* by limiting redundant information inherited from the source-node data.

However, directly computing  $I(Y_t; Z_H^{(L)})$  and  $I(\mathcal{D}_s; Z_H^{(L)})$  is generally intractable. Therefore, following variational techniques widely used in the IB principle [31] and GIB [30], we derive a tractable lower bound for  $I(Y_t; Z_H^{(L)})$  and an upper bound for  $I(\mathcal{D}_s; Z_H^{(L)})$ . These bounds are given in Proposition 1 and Proposition 2, respectively, with detailed derivations provided in Appendix A.

**Proposition 1.** For any variational distributions  $\mathbb{Q}_1(Y_t | Z_H^{(L)})$  and  $\mathbb{Q}_2(Y_t)$ , the mutual information  $I(Y_t; Z_H^{(L)})$  admits the following lower bound:

$$I(Y_t; Z_H^{(L)}) \geq 1 + \mathbb{E} \left[ \log \frac{\mathbb{Q}_1(Y_t | Z_H^{(L)})}{\mathbb{Q}_2(Y_t)} \right] - \mathbb{E}_{\mathbb{P}(Y_t)\mathbb{P}(Z_H^{(L)})} \left[ \frac{\mathbb{Q}_1(Y_t | Z_H^{(L)})}{\mathbb{Q}_2(Y_t)} \right]. \quad (7)$$

**Proposition 2.** For any variational distributions  $\mathbb{Q}(Z_H^{(l)})$  with  $l \in S_H$  and  $\mathbb{Q}(Z_A^{(l)})$  with  $l \in S_A$ , under the Markovian dependence space  $\mathcal{M}$ , the mutual information  $I(\mathcal{D}_s; Z_H^{(L)})$  admits the following upper bound:

$$I(\mathcal{D}_s; Z_H^{(L)}) \leq I(\mathcal{D}_s; \{Z_H^{(l)}\}_{l \in S_H} \cup \{Z_A^{(l)}\}_{l \in S_A}) \leq \sum_{l \in S_A} \text{AIB}^{(l)} + \sum_{l \in S_H} \text{HIB}^{(l)}, \quad (8)$$

$$\text{AIB}^{(l)} = \mathbb{E} \left[ \log \frac{\mathbb{P}(Z_A^{(l)} | A, Z_X^{(l)})}{\mathbb{Q}(Z_A^{(l)})} \right], \text{HIB}^{(l)} = \mathbb{E} \left[ \log \frac{\mathbb{P}(Z_H^{(l)} | Z_A^{(l)}, Z_X^{(l)})}{\mathbb{Q}(Z_H^{(l)})} \right],$$

where  $S_H$  and  $S_A$  satisfy: (1)  $S_H \subseteq \{0, 1, \dots, L\}$  and  $S_H \neq \emptyset$ ; (2)  $S_A = \{\max(S_H), \dots, L\}$ .

### 3.2 Instantiating the MLGIB Principle

In this section, we instantiate Proposition 1 & 2 as tractable learning objectives, yielding an end-to-end differentiable message-passing architecture. The overall instantiation is illustrated in Fig. 2.

#### 3.2.1 Instantiation of Proposition 1 (Lower Bound)

We start by instantiating the lower bound in Eq. 7, where for the first term, we have

$$\mathbb{E} \left[ \log \frac{\mathbb{Q}_1(Y_t | Z_H^{(L)})}{\mathbb{Q}_2(Y_t)} \right] = \mathbb{E} \left[ \log \mathbb{Q}_1(Y_t | Z_H^{(L)}) \right] - \mathbb{E} [\log \mathbb{Q}_2(Y_t)]. \quad (9)$$

We set  $\mathbb{Q}_2(Y_t)$  as the empirical label distribution  $\mathbb{P}(Y_t)$ . Then, the second term in Eq. 9 becomes

$$\mathbb{E} [\log \mathbb{Q}_2(Y_t)] = \int_Y \int_{Z_H^{(L)}} \mathbb{P}(Y_t, Z_H^{(L)}) \log \mathbb{P}(Y_t) dZ_H^{(L)} dY = \int_Y \mathbb{P}(Y_t) \log \mathbb{P}(Y_t) dY = \text{Const.} \quad (10)$$

Since this term depends only on the ground-truth label distribution, it is independent of model parameters and can be treated as a constant. Therefore,

$$\mathbb{E} \left[ \log \frac{\mathbb{Q}_1(Y_t | Z_H^{(L)})}{\mathbb{Q}_2(Y_t)} \right] = \mathbb{E} \left[ \log \mathbb{Q}_1(Y_t | Z_H^{(L)}) \right] - \text{Const.} \quad (11)$$

The second term of Eq. 7 is

$$\begin{aligned} \mathbb{E}_{\mathbb{P}(Y_t)\mathbb{P}(Z_H^{(L)})} \left[ \frac{\mathbb{Q}_1(Y_t | Z_H^{(L)})}{\mathbb{Q}_2(Y_t)} \right] &= \int_{Z_H^{(L)}} \int_Y \frac{\mathbb{Q}_1(Y_t | Z_H^{(L)})}{\mathbb{P}(Y_t)} \mathbb{P}(Y_t) \mathbb{P}(Z_H^{(L)}) dY dZ_H^{(L)} \\ &= \int_{Z_H^{(L)}} \mathbb{P}(Z_H^{(L)}) dZ_H^{(L)} = 1. \end{aligned} \quad (12)$$

Therefore, the lower bound in Proposition 1 can be simplified as

$$I(Y_t; Z_H^{(L)}) \geq \mathbb{E} \left[ \log \mathbb{Q}_1(Y_t | Z_H^{(L)}) \right] - \text{Const.} \quad (13)$$

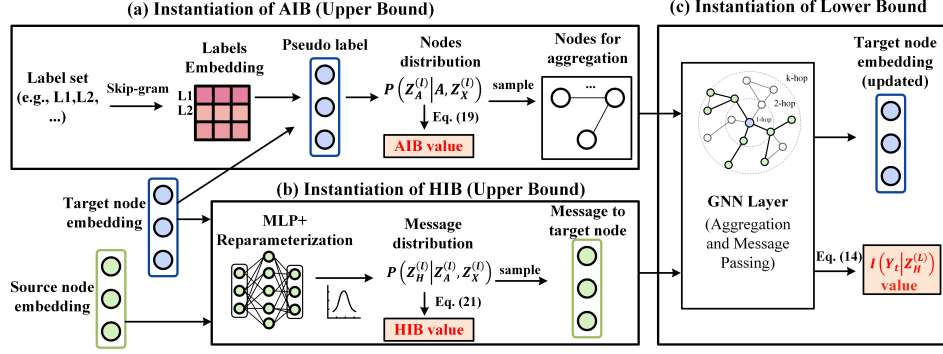


Figure 2: MLGIB is instantiated as a label-aware message-passing pipeline. (a) The instantiation of AIB learns label embeddings, derives pseudo labels, and samples label-relevant neighbors to constrain redundant structural information; (b) The instantiation of HIB parameterizes and samples transmitted messages to improve message purity. (c) The selected neighbors and purified messages are then aggregated in a GNN layer, instantiating the lower-bound objective and producing updated target-node embeddings that preserve predictive label signals.

We parameterize  $Q_1(Y_t | Z_H^{(L)})$  as an independent Bernoulli distribution over labels, reducing to:

$$-I(Y_t; Z_H^{(L)}) \rightarrow \sum_{v \in \mathcal{V}} \text{BCE}(y_v, \sigma(\text{Aggfunc}(z_{h,u \rightarrow v}^{(L)}))), \quad (14)$$

where BCE is the binary cross-entropy loss,  $\mathcal{V}$  is the node set,  $y_v$  is the multi-label ground-truth of node  $v$ , and  $z_{h,u \rightarrow v}^{(L)}$  is the message passed from node  $u$  to node  $v$  at layer  $L$ . The sigmoid function  $\sigma$  independently estimates the probability of each label. The aggregation function is defined as

$$\text{Aggfunc}(z_{h,u \rightarrow v}^{(L)}) = \sum_{u \in \alpha_v^{(L)}} W z_{h,u \rightarrow v}^{(L)}, \quad (15)$$

where  $\alpha_v^{(L)}$ , instantiated from  $Z_A^{(L)}$ , denotes the sampled message-passing neighborhood of node  $v$ , and  $W$  is a learnable matrix. Therefore, maximizing the lower bound enhances the expressiveness of MLGIB by encouraging the propagated messages to preserve predictive label information.

### 3.2.2 Instantiation of Proposition 2 (Upper Bound)

The upper bound of  $I(\mathcal{D}_s; Z_H^{(L)})$  consists of two terms:  $\text{AIB}^{(l)}$  for regulating message-passing paths and  $\text{HIB}^{(l)}$  for controlling message purity.

**Instantiation of AIB.** The first term in Proposition 2 is defined as  $\text{AIB}^{(l)} = \mathbb{E} \left[ \log \frac{\mathbb{P}(Z_A^{(l)} | A, Z_X^{(l)})}{\mathbb{Q}(Z_A^{(l)})} \right]$ ,

where  $Z_A^{(l)}$  denotes the sampled message-passing paths. In multi-label graphs, message-passing paths should favor label-relevant neighbors. Therefore, we parameterize  $\mathbb{P}(Z_A^{(l)} | A, Z_X^{(l)})$  using label correlations, so that paths connecting label-relevant nodes are assigned higher probabilities.

To capture label correlations, we learn label embeddings using a skip-gram objective [32] in training data. Let  $L_v$  be the label set of node  $v$ . For  $l_t \in L_v$ , we use  $L_v \setminus \{l_t\}$  as positive contexts and draw negatives  $l_n \in N(L_v)$ , where  $N(L_v)$  denotes  $K$  labels sampled from outside  $L_v$ .

$$\mathcal{L}_{\text{skip-gram}} = - \sum_{v \in \mathcal{V}} \left[ \sum_{l_c \in L_v \setminus \{l_t\}} \log \sigma(\text{emb}(l_c)^\top \text{emb}(l_t)) + \sum_{l_n \in N(L_v)} \log \sigma(-\text{emb}(l_n)^\top \text{emb}(l_t)) \right], \quad (16)$$

where  $\text{emb}(\cdot)$  is the embedding function. This yields a dictionary  $\mathcal{D}_L \in \mathbb{R}^{C \times d}$ , containing embeddings for all labels, where  $C$  is the number of labels and  $d$  is the dimension. For each node  $v$ , we construct a label-aware representation

$$z_{p,v}^{(l)} = \text{MLP}(z_{x,v}^{(l)})^\top \mathcal{D}_L, \text{MLP}(z_{x,v}^{(l)}) \in \mathbb{R}^C, \quad (17)$$

where  $z_{x,v}^{(l)}$  is the layer- $l$  node representation. The probability of selecting node  $u$  as a message-passing neighbor of node  $v$  is then defined as

$$\mathbb{P}(Z_A^{(l)} = (v, u) \mid A, Z_X^{(l)}) = \frac{\exp((z_{p,v}^{(l)})^\top z_{p,u}^{(l)})}{\sum_{i \in \mathcal{N}_v} \exp((z_{p,v}^{(l)})^\top z_{p,i}^{(l)})}, \quad (18)$$

where  $u \in \mathcal{N}_v$ ,  $\mathcal{N}_v$  is the 1-hop neighbor nodes of node  $v$ , and  $|\mathcal{N}_v|$  denotes the number of neighbors. We further set  $Q(Z_A^{(l)})$  to be a uniform distribution [30] for regularization, which yield

$$\text{AIB}^{(l)} \rightarrow \sum_{v \in \mathcal{V}} \sum_{u \in \mathcal{N}_v} \left( \log \frac{\exp((z_{p,v}^{(l)})^\top z_{p,u}^{(l)})}{\sum_{i \in \mathcal{N}_v} \exp((z_{p,v}^{(l)})^\top z_{p,i}^{(l)})} - \log \frac{1}{|\mathcal{N}_v|} \right). \quad (19)$$

**Instantiation of HIB.** The second term in 2 is defined as  $\text{HIB}^{(l)} = \mathbb{E} \left[ \log \frac{\mathbb{P}(Z_H^{(l)} \mid Z_A^{(l)}, Z_X^{(l)})}{\mathbb{Q}(Z_H^{(l)})} \right]$ .

Following the modeling strategy widely used in the Information Bottleneck literature [31, 30, 29], we start by modeling  $\mathbb{Q}(Z_H^{(l)})$  via a Gaussian mixture distribution for node  $v$  and node  $u$ , i.e.,

$$\mathbb{Q}(Z_H^{(l)}) \rightarrow \sum_{i=1}^m w_i \Phi(z_{h,v \rightarrow u}^{(l)}; \mu_i; \sigma_i^2), \text{ where } w_i, \mu_i \text{ and } \sigma_i^2 \text{ are learnable parameters, and } \Phi(\cdot)$$

denotes a Gaussian density. To enable stochastic optimization of  $\mathbb{P}(Z_H^{(l)} \mid Z_A^{(l)}, Z_X^{(l)})$ , we model it as a Gaussian distribution parameterized by neural networks, and apply the reparameterization trick [33] for sampling:  $z_{h,v \rightarrow u}^{(l)} = \mu_{v,u}^{(l)} + \sigma_{v,u}^{(l)} \cdot \epsilon$ ,  $\epsilon \sim \mathcal{N}(0, I)$ , where

$$\mu_{v,u}^{(l)} = \text{MLP}_1(z_{x,v}^{(l)} \parallel z_{x,u}^{(l)}), \quad \sigma_{v,u}^{(l)} = \text{MLP}_2(z_{x,v}^{(l)} \parallel z_{x,u}^{(l)}), \quad (20)$$

and  $\parallel$  denotes concatenation. By concatenating the two nodes and applying two separate MLPs, we obtain the mean and variance of the message sent from node  $v$  to node  $u$ , yielding HIB as follows:

$$\text{HIB}^{(l)} \rightarrow \sum_{v \in \mathcal{V}} \sum_{u \in \alpha_v^{(l)}} \left[ \log \Phi(z_{h,v \rightarrow u}^{(l)}; \mu_{v,u}^{(l)}; \sigma_{v,u}^{(l)}) - \log \sum_{i=1}^m w_i \Phi(z_{h,v \rightarrow u}^{(l)}; \mu_i; \sigma_i^2) \right]. \quad (21)$$

Finally, substituting the instantiated results of AIB and HIB back into Eq. 8. By minimizing this upper bound, MLGIB constrains redundant information from the source graph, thereby improving robustness against irrelevant label noise during multi-label message passing.

## 4 Experiment

### 4.1 Experiment Setup

**Dataset.** We conduct experiments on four real-world multi-label datasets including DBLP [34], BlogCatalog [35], PCG [36] and Delve [23]. Details are provided in Appendix C.1.

**Baseline Models.** We compare MLGIB with four categories of baselines: representative GNNs, including GCN [37] and GAT [38]; the graph application of the IB principle, GIB [30]; over-squashing mitigation methods based on graph rewiring, including SDRF [7], FOSR [25], and BORF [26]; and the state-of-the-art multi-label graph method CorGCN [15].

**Evaluation Metrics.** We evaluate MLGIB using seven metrics: Macro-AUC, Micro-AUC, Ranking Loss, Hamming Loss, Macro-AP, Micro-AP, and LRAP. Details are provided in Appendix C.2.

### 4.2 Performance Evaluation

Table 1 reports the node classification results, with best results in bold. We summarize two observations: (1) **Superiority of MLGIB on multi-label graphs.** Its improvement over GIB shows that the information bottleneck principle needs to be tailored to multi-label message passing, while its advantage over CorGCN highlights that modeling label correlations alone is insufficient, and that preserving predictive information during propagation is equally important. (2) **Effectiveness of MLGIB against multi-label over-squashing.** Rewiring methods (SDRF, FOSR, and BORF) provide limited gains and may suffer scalability issues, suggesting that denser or modified connectivity can amplify label noise in multi-label graphs. By contrast, MLGIB regulates information flow without altering the graph structure, achieving a better balance between expressiveness and robustness.

Table 1: Node classification results on multiple real-world datasets using various metrics.

Dataset	Model	Macro-AUC	Micro-AUC	Ranking Loss	Hamming Loss	Macro-AP	Micro-AP	LRAP
DBLP	GCN	0.9485 ± 0.0005	0.9527 ± 0.0004	0.0510 ± 0.0004	0.0883 ± 0.0007	0.9049 ± 0.0007	0.9214 ± 0.0004	0.9447 ± 0.0005
	GAT	0.9501 ± 0.0023	0.9540 ± 0.0016	0.0575 ± 0.0009	0.0944 ± 0.0014	0.8901 ± 0.0043	0.9123 ± 0.0014	0.9387 ± 0.0008
	GIB	0.9478 ± 0.0026	0.9517 ± 0.0025	0.0636 ± 0.0039	0.0989 ± 0.0040	0.8868 ± 0.0066	0.9079 ± 0.0055	0.9319 ± 0.0047
	FOSR	0.9486 ± 0.0006	0.9527 ± 0.0005	0.0515 ± 0.0009	0.0886 ± 0.0010	0.9052 ± 0.0008	0.9215 ± 0.0008	0.9442 ± 0.0010
	SDRF	0.9487 ± 0.0005	0.9528 ± 0.0004	0.0509 ± 0.0004	0.0884 ± 0.0005	0.9050 ± 0.0005	0.9215 ± 0.0003	0.9448 ± 0.0005
	BORF	0.9477 ± 0.0005	0.9520 ± 0.0004	0.0520 ± 0.0005	0.0885 ± 0.0007	0.9031 ± 0.0008	0.9199 ± 0.0005	0.9437 ± 0.0007
	CORGCN	0.9504 ± 0.0004	0.9545 ± 0.0004	0.0699 ± 0.0005	0.0983 ± 0.0009	0.8926 ± 0.0016	0.9134 ± 0.0010	0.9226 ± 0.0006
	<b>MLGIB(ours)</b>	<b>0.9699 ± 0.0008</b>	<b>0.9716 ± 0.0007</b>	<b>0.0441 ± 0.0012</b>	<b>0.0664 ± 0.0011</b>	<b>0.9356 ± 0.0018</b>	<b>0.9464 ± 0.0012</b>	<b>0.9531 ± 0.0012</b>
BlogCatalog	GCN	0.4617 ± 0.0017	0.6348 ± 0.0037	0.2608 ± 0.0037	0.0358 ± 0.0003	0.0360 ± 0.0005	0.0558 ± 0.0022	0.2604 ± 0.0110
	GAT	0.5356 ± 0.0135	0.7435 ± 0.0026	0.2550 ± 0.0025	0.0353 ± 0.0003	0.0497 ± 0.0065	0.1039 ± 0.0163	0.2747 ± 0.0114
	GIB	0.5229 ± 0.0105	0.7394 ± 0.0005	0.2579 ± 0.0004	0.0355 ± 0.0000	0.0463 ± 0.0045	0.0906 ± 0.0029	0.2645 ± 0.0008
	FOSR	0.4619 ± 0.0016	0.6333 ± 0.0024	0.2618 ± 0.0036	0.0357 ± 0.0002	0.0359 ± 0.0003	0.0558 ± 0.0026	0.2556 ± 0.0119
	SDRF	0.4621 ± 0.0019	0.6347 ± 0.0043	0.2615 ± 0.0037	0.0359 ± 0.0005	0.0361 ± 0.0005	0.0558 ± 0.0025	0.2572 ± 0.0134
	BORF	OOM	OOM	OOM	OOM	OOM	OOM	OOM
	CORGCN	0.5207 ± 0.0095	0.7384 ± 0.0004	0.2588 ± 0.0004	0.0355 ± 0.0000	0.0422 ± 0.0010	0.0884 ± 0.0008	0.2638 ± 0.0003
	<b>MLGIB(ours)</b>	<b>0.5627 ± 0.0148</b>	<b>0.7527 ± 0.0022</b>	<b>0.2453 ± 0.0022</b>	<b>0.0347 ± 0.0004</b>	<b>0.0691 ± 0.0080</b>	<b>0.1430 ± 0.0151</b>	<b>0.3049 ± 0.0110</b>
PCG	GCN	0.4676 ± 0.0051	0.6265 ± 0.0025	0.2634 ± 0.0034	0.1358 ± 0.0004	0.1491 ± 0.0025	0.2256 ± 0.0049	0.4826 ± 0.0058
	GAT	0.5220 ± 0.0206	0.6803 ± 0.0136	0.2898 ± 0.0124	0.1431 ± 0.0035	0.1501 ± 0.0083	0.2326 ± 0.0146	0.4557 ± 0.0139
	GIB	0.5195 ± 0.0085	0.6927 ± 0.0086	0.2783 ± 0.0081	0.1364 ± 0.0006	0.1467 ± 0.0029	0.2496 ± 0.0072	0.4689 ± 0.0072
	FOSR	0.4738 ± 0.0068	0.6299 ± 0.0037	0.2621 ± 0.0041	0.1356 ± 0.0007	0.1508 ± 0.0029	0.2293 ± 0.0046	0.4838 ± 0.0055
	SDRF	0.4677 ± 0.0052	0.6266 ± 0.0025	0.2634 ± 0.0034	0.1358 ± 0.0004	0.1492 ± 0.0026	0.2258 ± 0.0049	0.4828 ± 0.0057
	BORF	0.5122 ± 0.0038	0.6443 ± 0.0024	0.2817 ± 0.0024	0.1381 ± 0.0006	0.1459 ± 0.0025	0.2217 ± 0.0042	0.4606 ± 0.0042
	CORGCN	0.5571 ± 0.0177	0.7083 ± 0.0053	0.2647 ± 0.0013	0.1357 ± 0.0001	0.1797 ± 0.0075	0.2777 ± 0.0051	0.4816 ± 0.0033
	<b>MLGIB(ours)</b>	<b>0.6005 ± 0.0051</b>	<b>0.7252 ± 0.0021</b>	<b>0.2619 ± 0.0024</b>	<b>0.1356 ± 0.0001</b>	<b>0.2079 ± 0.0061</b>	<b>0.2951 ± 0.0055</b>	<b>0.4844 ± 0.0052</b>
Delve	GCN	0.7110 ± 0.0075	0.8098 ± 0.0042	0.0091 ± 0.0003	0.0069 ± 0.0000	0.0699 ± 0.0027	0.1195 ± 0.0030	0.9713 ± 0.0007
	GAT	0.8931 ± 0.0020	0.9263 ± 0.0009	0.0084 ± 0.0001	0.0065 ± 0.0000	0.1050 ± 0.0032	0.1854 ± 0.0030	0.9740 ± 0.0003
	CORGCN	0.9541 ± 0.0011	0.9686 ± 0.0003	0.0039 ± 0.0000	0.0061 ± 0.0000	0.2548 ± 0.0062	0.3404 ± 0.0018	0.9854 ± 0.0001
	<b>MLGIB(ours)</b>	<b>0.9867 ± 0.0003</b>	<b>0.9903 ± 0.0001</b>	<b>0.0012 ± 0.0000</b>	<b>0.0056 ± 0.0001</b>	<b>0.4414 ± 0.0055</b>	<b>0.5334 ± 0.0052</b>	<b>0.9940 ± 0.0001</b>

“OOM” stands for Out Of Memory. The implementations provided of FOSR, SDRF, BORF and GIB are not adapted for the large graph Delve.

### 4.3 Expressiveness Analysis

To evaluate whether MLGIB can preserve informative label signals under multi-label interference, we analyze its expressiveness from two complementary perspectives: label-wise expressiveness on multi-label graphs and cross-setting expressiveness on single-label graphs.

#### 4.3.1 Label-wise Expressiveness on Multi-label Graphs

We conduct label-wise evaluations on Delve, DBLP, and PCG. As shown in Fig. 3a, MLGIB outperforms CorGCN on most labels, showing that it consistently preserves predictive signals across labels instead of only improving dominant or highly correlated ones. These results indicate stronger expressiveness in extracting label-specific informative signals from noisy multi-label propagation.

#### 4.3.2 Cross-setting Expressiveness on Single-label Graphs

We evaluate MLGIB on the single-label PubMed dataset [39], where nodes represent biomedical articles and edges denote citation links. Details are provided in Appendix C.1. As shown in Fig. 3b, MLGIB does not degrade in the single-label setting and even outperforms GCN and CorGCN. This demonstrates that MLGIB enhances the intrinsic expressiveness of message passing rather than overfitting to multi-label-specific patterns.

### 4.4 Robustness Analysis

We further evaluate the robustness of MLGIB under challenging conditions where irrelevant label signals are likely to be amplified.

#### 4.4.1 Robustness under Low Label Correlation

In multi-label node classification, lower label correlation between neighboring nodes usually indicates higher aggregation noise, as irrelevant label signals are more likely to interfere with predictive ones. To quantify this effect, we compute the average Jaccard similarity [40] between each node’s label set and those of its neighbors. As shown in Fig. 4, on the large graph Delve, classification performance generally decreases as neighbor-label similarity becomes lower. However, MLGIB exhibits a slower performance degradation and more stable fluctuations than the baselines, demonstrating its robustness

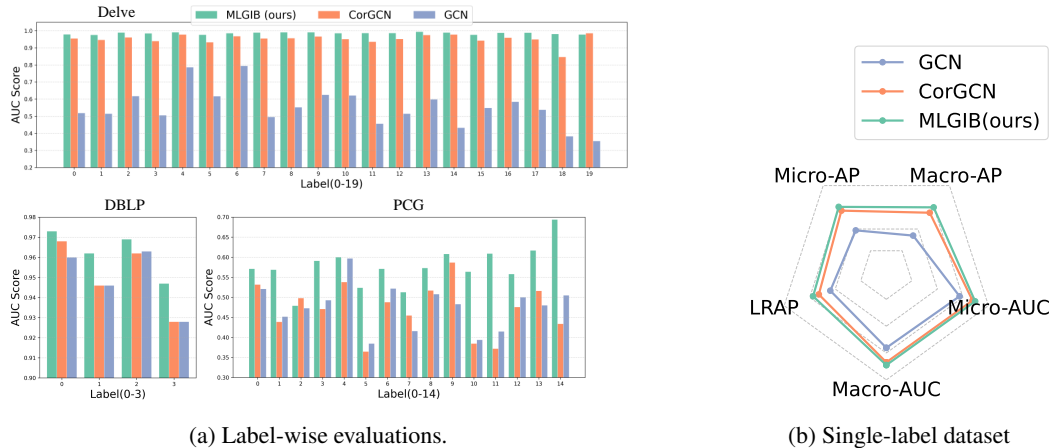


Figure 3: (a) Expressiveness Analysis (AUC) is conducted for each label on the Delve, DBLP, and PCG datasets, respectively. (b) Cross-setting Expressiveness on Single-label Graphs PubMed.

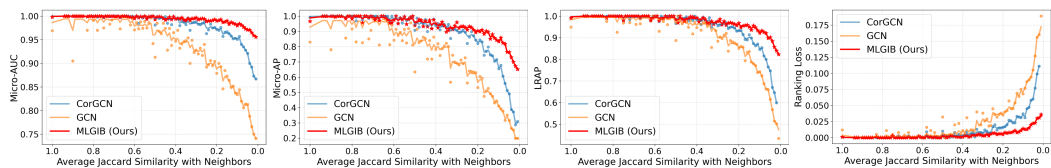


Figure 4: Impact of decreased Jaccard similarity with neighbor nodes on performance. Dots denote true values and lines denote fitted trends.

against weak label correlation and its ability to suppress irrelevant label noise during message passing.

#### 4.4.2 Robustness under High Node Degree

Node degree has a dual effect on multi-label message passing. A larger neighborhood may provide richer context, but also introduce more irrelevant messages, increasing aggregation noise and aggravating over-squashing. As shown in Fig. 5, LRAP decreases and Hamming Loss increases with node degree of Delve dataset, indicating that high-degree nodes are more vulnerable to noisy aggregation. Compared with baselines, MLGIB shows much smaller performance degradation, suggesting that its information-filtering mechanism improves robustness to noisy and excessively large neighborhoods.

#### 4.4.3 Robustness Analysis on Structural Perturbations

Beyond inherent graph properties, we further evaluate robustness by actively injecting structural noise. We conduct this experiment on DBLP, whose clear structural semantics make it suitable for assessing the impact of perturbations on multi-label aggregation. Specifically, we randomly add edges according to a proportion of the original edge count, ranging from 0 to 1; when the proportion reaches 1, the graph contains twice as many edges as the original. As shown in Fig. 6, all models

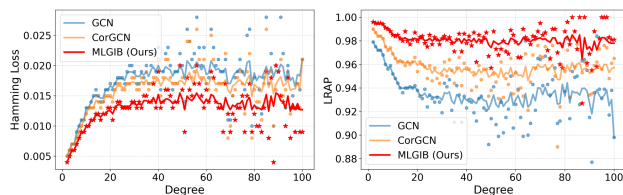


Figure 5: Impact of increased node degree on performance, where dots and lines follow Fig. 4.

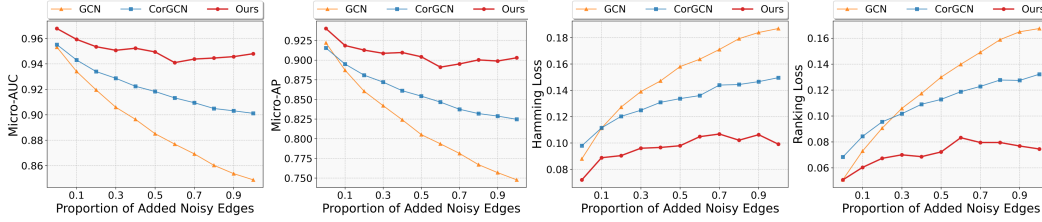


Figure 6: Impact of added noisy edges on performance.

Table 2: The results of ablation study.

Dataset	Model	Macro-AUC	Micro-AUC	Ranking Loss	Hamming Loss	Macro-AP	Micro-AP	LRAP
DBLP	MLGIB	<b>0.9699 ± 0.0008</b>	<b>0.9716 ± 0.0007</b>	<b>0.0441 ± 0.0012</b>	<b>0.0664 ± 0.0011</b>	<b>0.9356 ± 0.0018</b>	<b>0.9464 ± 0.0012</b>	<b>0.9531 ± 0.0012</b>
	w/o AIB Instantiation	0.9589 ± 0.0023	0.9616 ± 0.0018	0.0588 ± 0.0026	0.0852 ± 0.0028	0.9129 ± 0.0048	0.9273 ± 0.0034	0.9366 ± 0.0030
	w/o HIB Instantiation	0.9458 ± 0.0055	0.9508 ± 0.0046	0.0581 ± 0.0036	0.0957 ± 0.0029	0.8861 ± 0.0082	0.9095 ± 0.0058	0.9378 ± 0.0035
BlogCatalog	MLGIB	<b>0.5627 ± 0.0148</b>	<b>0.7527 ± 0.0022</b>	<b>0.2453 ± 0.0022</b>	<b>0.0347 ± 0.0004</b>	<b>0.0691 ± 0.0080</b>	<b>0.1430 ± 0.0151</b>	<b>0.3049 ± 0.0110</b>
	w/o AIB Instantiation	0.5116 ± 0.0065	0.7387 ± 0.0004	0.2582 ± 0.0001	0.0355 ± 0.0000	0.0427 ± 0.0029	0.0888 ± 0.0013	0.2637 ± 0.0005
	w/o HIB Instantiation	0.5013 ± 0.0153	0.7202 ± 0.0053	0.2749 ± 0.0054	0.0355 ± 0.0000	0.0404 ± 0.0031	0.0819 ± 0.0035	0.2520 ± 0.0090
PCG	MLGIB	<b>0.6005 ± 0.0051</b>	<b>0.7252 ± 0.0021</b>	<b>0.2619 ± 0.0024</b>	<b>0.1356 ± 0.0001</b>	<b>0.2079 ± 0.0061</b>	<b>0.2951 ± 0.0055</b>	<b>0.4844 ± 0.0052</b>
	w/o AIB Instantiation	0.5475 ± 0.0144	0.7079 ± 0.0023	0.2678 ± 0.0015	0.1356 ± 0.0003	0.1610 ± 0.0076	0.2718 ± 0.0072	0.4775 ± 0.0055
	w/o HIB Instantiation	0.5233 ± 0.0101	0.6629 ± 0.0105	0.3051 ± 0.0092	0.1477 ± 0.0044	0.1488 ± 0.0029	0.2174 ± 0.0083	0.4428 ± 0.0099
Delve	MLGIB	<b>0.9867 ± 0.0003</b>	<b>0.9903 ± 0.0001</b>	<b>0.0012 ± 0.0000</b>	<b>0.0056 ± 0.0001</b>	<b>0.4414 ± 0.0055</b>	<b>0.5334 ± 0.0052</b>	<b>0.9940 ± 0.0001</b>
	w/o AIB Instantiation	0.9493 ± 0.0037	0.9711 ± 0.0007	0.0024 ± 0.0001	0.0063 ± 0.0000	0.2578 ± 0.0044	0.3602 ± 0.0042	0.9906 ± 0.0002
	w/o HIB Instantiation	0.8825 ± 0.0040	0.9177 ± 0.0029	0.0082 ± 0.0002	0.0065 ± 0.0000	0.1050 ± 0.0046	0.1786 ± 0.0063	0.9738 ± 0.0005

degrade as more random edges are added, but MLGIB exhibits the slowest degradation. This confirms that MLGIB is robust to structural perturbations by filtering irrelevant information from noisy edges, thereby mitigating multi-label over-squashing caused by rapidly expanding information sources.

#### 4.5 Ablation Study

We conduct an ablation study to evaluate the contribution of each component in MLGIB, by fixing the instantiation of the lower bound and replacing the instantiation of AIB and HIB with the original graph structure  $A$  and node embeddings  $Z_X^{(l)}$ , respectively. Table 2 shows: (1) **Both components are essential.** Removing either leads to consistent performance degradation, demonstrating that both informative message-passing paths and purified messages are necessary for effective multi-label message passing. (2) **Effect of removing AIB Instantiation.** Without it, MLGIB lacks the constraint on redundant message paths from source-node data, increasing the difficulty of message purification when there are many redundant paths. (3) **Effect of removing HIB Instantiation.** Without it, performance drops significantly, especially on the Delve dataset, further strengthening our insight: **In multi-label graphs, over-squashing is not merely caused by structural constraints, but by whether informative signals can be extracted from partially overlapping label information.** This demonstrates that we have substantially alleviated over-squashing in multi-label graphs.

## 5 Conclusion

In this paper, we investigated over-squashing in multi-label graphs, where message passing not only compresses long-range information but also mixes predictive label signals with irrelevant noise caused by partial label overlap. To address this issue, we proposed the MLGIB, which formulates multi-label message passing as constrained information transmission. By balancing expressiveness and robustness, MLGIB preserves predictive label signals while suppressing irrelevant noise through tractable variational bounds and an end-to-end differentiable architecture. Experiments on real-world multi-label datasets show that MLGIB consistently outperforms representative GNNs, graph rewiring methods, graph information bottleneck methods, and state-of-the-art multi-label graph models.

## References

- [1] Niloofar Azizi, Nils M. Kriege, Nicholas J. A. Harvey, and Horst Bischof. Spectral basis learning for expressive graph neural networks in link prediction. In *AAAI*, pages 19640–19648. AAAI Press, 2026.
- [2] Asela Hevopathige, Asiri Wijesinghe, and Ahad N. Zehmakan. Beyond fixed depth: Adaptive graph neural networks for node classification under varying homophily. In *AAAI*, pages 21717–21725. AAAI Press, 2026.
- [3] Lihui Liu and Yuchen Yan. MORGAN: to bridge mixture of experts and spectral graph neural network. In *AAAI*, pages 23783–23791. AAAI Press, 2026.
- [4] Richard Bergna, Sergio Calvo-Ordoñez, Felix L. Opolka, Pietro Lio, and José Miguel Hernández-Lobato. Uncertainty modeling in graph neural networks via stochastic differential equations. In *ICLR*. OpenReview.net, 2025.
- [5] Shouheng Li, Floris Geerts, Dongwoo Kim, and Qing Wang. Towards bridging generalization and expressivity of graph neural networks. In *ICLR*. OpenReview.net, 2025.
- [6] Uri Alon and Eran Yahav. On the bottleneck of graph neural networks and its practical implications. In *ICLR 2021, Virtual Event, Austria, May 3-7, 2021*. OpenReview.net, 2021.
- [7] Jake Topping, Francesco Di Giovanni, Benjamin Paul Chamberlain, Xiaowen Dong, and Michael M. Bronstein. Understanding over-squashing and bottlenecks on graphs via curvature. In *ICLR 2022, Virtual Event, April 25-29, 2022*. OpenReview.net, 2022.
- [8] Adarsh Jamadandi, Celia Rubio-Madrigal, and Rebekka Burkholz. Spectral graph pruning against over-squashing and over-smoothing. In *NeurIPS*, 2024.
- [9] Jiong Zhu, Yujun Yan, Lingxiao Zhao, Mark Heimann, Leman Akoglu, and Danai Koutra. Beyond homophily in graph neural networks: Current limitations and effective designs. In *NeurIPS*, 2020.
- [10] Zengyi Wo, Minglai Shao, Shiyu Zhang, and Ruijie Wang. Local homophily-aware graph neural network with adaptive polynomial filters for scalable graph anomaly detection. In *Proceedings of the 31st ACM SIGKDD Conference on Knowledge Discovery and Data Mining V. 2*, pages 3180–3191, 2025.
- [11] Donald Loveland and Danai Koutra. Unveiling the impact of local homophily on gnn fairness: In-depth analysis and new benchmarks. In *Proceedings of the 2025 SIAM International Conference on Data Mining (SDM)*, pages 608–617. SIAM, 2025.
- [12] Yan Jiang, Ruihong Qiu, and Zi Huang. Does homophily help in robust test-time node classification? In *Proceedings of the Nineteenth ACM International Conference on Web Search and Data Mining*, pages 271–281, 2026.
- [13] Hsiang-Fu Yu, Prateek Jain, Purushottam Kar, and Inderjit Dhillon. Large-scale multi-label learning with missing labels. In *International conference on machine learning*, pages 593–601. PMLR, 2014.
- [14] Kush Bhatia, Himanshu Jain, Purushottam Kar, Manik Varma, and Prateek Jain. Sparse local embeddings for extreme multi-label classification. *Advances in neural information processing systems*, 28, 2015.
- [15] Yuanchen Bei, Weizhi Chen, Hao Chen, Sheng Zhou, Carl Yang, Jiapei Fan, Longtao Huang, and Jiajun Bu. Correlation-aware graph convolutional networks for multi-label node classification. In *Proceedings of the 31st ACM SIGKDD Conference on Knowledge Discovery and Data Mining V. 1*, pages 37–48, 2025.
- [16] Jiayang Wu, Wensheng Gan, Huashen Lu, and Philip S Yu. Graph contrastive learning on multi-label classification for recommendations. *ACM Transactions on Intelligent Systems and Technology*, 16(4):1–19, 2025.

- [17] Yifei Sun, Zemin Liu, Bryan Hooi, Yang Yang, Rizal Fathony, Jia Chen, and Bingsheng He. Multi-label node classification with label influence propagation. In *The Thirteenth International Conference on Learning Representations*, 2025.
- [18] Yiyuan Chen, Donghai Guan, Weiwei Yuan, and Tianzi Zang. Beyond homophily: Graph contrastive learning with macro-micro message passing. In *Proceedings of the AAAI Conference on Artificial Intelligence*, volume 39(15), pages 15948–15956, 2025.
- [19] Przemysław Andrzej Wałęga and Michael Rawson. Expressive power of temporal message passing. In *Proceedings of the AAAI Conference on Artificial Intelligence*, volume 39(20), pages 21000–21008, 2025.
- [20] Langzhang Liang, Fanchen Bu, Zixing Song, Zenglin Xu, Shirui Pan, and Kijung Shin. Mitigating over-squashing in graph neural networks by spectrum-preserving sparsification. In *ICML, Proceedings of Machine Learning Research*. PMLR / OpenReview.net, 2025.
- [21] Danial Saber and Amirali Salehi-Abari. Empirical study of over-squashing in gnns and causal estimation of rewiring strategies. In *CIKM*, pages 2525–2534. ACM, 2025.
- [22] Cangqi Zhou, Hui Chen, Jing Zhang, Qianmu Li, Dianming Hu, and Victor S Sheng. Multi-label graph node classification with label attentive neighborhood convolution. *Expert Systems with Applications*, 180:115063, 2021.
- [23] Lin Xiao, Pengyu Xu, Liping Jing, Uchenna Akujuobi, and Xiangliang Zhang. Semantic guide for semi-supervised few-shot multi-label node classification. *Information Sciences*, 591: 235–250, 2022.
- [24] Kaisheng Gao, Jing Zhang, and Cangqi Zhou. Semi-supervised graph embedding for multi-label graph node classification. In *International Conference on Web Information Systems Engineering*, pages 555–567. Springer, 2019.
- [25] Kedar Karhadkar, Pradeep Banerjee, and Guido Montufar. Fosr: First-order spectral rewiring for addressing oversquashing in gnns. In *International Conference on Learning Representations*, 2023.
- [26] Khang Nguyen, Nong Minh Hieu, Vinh Duc Nguyen, Nhat Ho, Stanley Osher, and Tan Minh Nguyen. Revisiting over-smoothing and over-squashing using ollivier-ricci curvature. In *International Conference on Machine Learning*, pages 25956–25979. PMLR, 2023.
- [27] Naftali Tishby, Fernando C Pereira, and William Bialek. The information bottleneck method. *arXiv preprint physics/0004057*, 2000.
- [28] Naftali Tishby and Noga Zaslavsky. Deep learning and the information bottleneck principle. In *2015 IEEE Information Theory Workshop (ITW)*, pages 1–5. Ieee, 2015.
- [29] Andrew M Saxe, Yamini Bansal, Joel Dapello, Madhu Advani, Artemy Kolchinsky, Brendan D Tracey, and David D Cox. On the information bottleneck theory of deep learning. *Journal of Statistical Mechanics: Theory and Experiment*, 2019(12):124020, 2019.
- [30] Tailin Wu, Hongyu Ren, Pan Li, and Jure Leskovec. Graph information bottleneck. *Advances in Neural Information Processing Systems*, 33:20437–20448, 2020.
- [31] Alexander A Alemi, Ian Fischer, Joshua V Dillon, and Kevin Murphy. Deep variational information bottleneck. In *International Conference on Learning Representations*, 2017.
- [32] Tomas Mikolov, Ilya Sutskever, Kai Chen, Greg S Corrado, and Jeff Dean. Distributed representations of words and phrases and their compositionality. *Advances in neural information processing systems*, 26, 2013.
- [33] Diederik P. Kingma and Max Welling. Auto-encoding variational bayes. In *International Conference on Learning Representations (ICLR)*, 2014.
- [34] Uchenna Akujuobi, Han Yufei, Qiannan Zhang, and Xiangliang Zhang. Collaborative graph walk for semi-supervised multi-label node classification. In *2019 IEEE International Conference on Data Mining (ICDM)*, pages 1–10. IEEE, 2019.

- [35] Geetika Lakshmanan and Martin Oberhofer. Knowledge discovery in the blogosphere: Approaches and challenges. *IEEE internet computing*, 14(2):24–32, 2010.
- [36] Tianqi Zhao, Ngan Thi Dong, Alan Hanjalic, and Megha Khosla. Multi-label node classification on graph-structured data. *arXiv preprint arXiv:2304.10398*, 2023.
- [37] Thomas N. Kipf and Max Welling. Semi-supervised classification with graph convolutional networks. In *5th International Conference on Learning Representations, ICLR 2017, Toulon, France, April 24-26, 2017, Conference Track Proceedings*. OpenReview.net, 2017. URL <https://openreview.net/forum?id=SJU4ayYg1>.
- [38] Petar Veličković, Guillem Cucurull, Arantxa Casanova, Adriana Romero, Pietro Liò, and Yoshua Bengio. Graph attention networks. In *International Conference on Learning Representations*, 2018.
- [39] Prithviraj Sen, Galileo Namata, Mustafa Bilgic, Lise Getoor, Brian Galligher, and Tina Eliassi-Rad. Collective classification in network data. *AI magazine*, 29(3):93–93, 2008.
- [40] Paul Jaccard. The distribution of the flora in the alpine zone. 1. *New phytologist*, 11(2):37–50, 1912.
- [41] XuanLong Nguyen, Martin J Wainwright, and Michael I Jordan. Estimating divergence functionals and the likelihood ratio by convex risk minimization. *IEEE Transactions on Information Theory*, 56(11):5847–5861, 2010.
- [42] Thomas M. Cover and Joy A. Thomas. *Elements of information theory*. John Wiley & Sons, 2012.

## A Theoretical Supplement

### A.1 Proof of Proposition 1

*Proof.* To derive the lower bound of the mutual information  $I(Y_t; Z_H^{(L)})$ , we utilize the Nguyen-Wainwright-Jordan lower bound [41]. For any two distributions  $p(X)$  and  $q(X)$ :

$$\text{KL}(p||q) = \sup_g \left( \mathbb{E}_{p(X)}[g(X)] - \mathbb{E}_{q(X)}[\exp(g(X) - 1)] \right). \quad (22)$$

Recall that  $I(Y_t; Z_H^{(L)}) = \text{KL}(\mathbb{P}(Y_t, Z_H^{(L)}) \parallel \mathbb{P}(Y_t)\mathbb{P}(Z_H^{(L)}))$ , for any measurable function  $g(Y_t, Z_H^{(L)})$ , we have:

$$I(Y_t; Z_H^{(L)}) \geq \mathbb{E}_{\mathbb{P}(Y_t, Z_H^{(L)})}[g(Y_t, Z_H^{(L)})] - \mathbb{E}_{\mathbb{P}(Y_t)\mathbb{P}(Z_H^{(L)})}[\exp(g(Y_t, Z_H^{(L)}) - 1)]. \quad (23)$$

Define the variational function  $g(Y_t, Z_H^{(L)}) = 1 + \log \frac{\mathbb{Q}_1(Y_t | Z_H^{(L)})}{\mathbb{Q}_2(Y_t)}$ . Substituting this into the inequality, the first term becomes:

$$\mathbb{E}_{\mathbb{P}(Y_t, Z_H^{(L)})} \left[ 1 + \log \frac{\mathbb{Q}_1(Y_t | Z_H^{(L)})}{\mathbb{Q}_2(Y_t)} \right] = 1 + \mathbb{E}_{\mathbb{P}(Y_t, Z_H^{(L)})} \left[ \log \frac{\mathbb{Q}_1(Y_t | Z_H^{(L)})}{\mathbb{Q}_2(Y_t)} \right]. \quad (24)$$

The second term simplifies as:

$$\mathbb{E}_{\mathbb{P}(Y_t)\mathbb{P}(Z_H^{(L)})} \left[ \exp\left(1 + \log \frac{\mathbb{Q}_1(Y_t | Z_H^{(L)})}{\mathbb{Q}_2(Y_t)}\right) - 1 \right] = \mathbb{E}_{\mathbb{P}(Y_t)\mathbb{P}(Z_H^{(L)})} \left[ \frac{\mathbb{Q}_1(Y_t | Z_H^{(L)})}{\mathbb{Q}_2(Y_t)} \right]. \quad (25)$$

Combining these, we arrive at the lower bound:

$$I(Y_t; Z_H^{(L)}) \geq 1 + \mathbb{E}_{\mathbb{P}(Y_t, Z_H^{(L)})} \left[ \log \frac{\mathbb{Q}_1(Y_t | Z_H^{(L)})}{\mathbb{Q}_2(Y_t)} \right] - \mathbb{E}_{\mathbb{P}(Y_t)\mathbb{P}(Z_H^{(L)})} \left[ \frac{\mathbb{Q}_1(Y_t | Z_H^{(L)})}{\mathbb{Q}_2(Y_t)} \right], \quad (26)$$

which concludes the proof.  $\square$

## A.2 Proof of Proposition 2

*Proof.* Considering the source data  $\mathcal{D}_s = (A, X)$  and the Markovian dependence of  $\mathcal{M}$ , we establish the Markov chain:

$$\mathcal{D}_s \rightarrow \{Z_H^{(l)}\}_{l \in S_H} \cup \{Z_A^{(l)}\}_{l \in S_A} \rightarrow Z_H^{(L)}.$$

By the Data Processing Inequality [42], the upper bound of the target term is:

$$I(\mathcal{D}_s; Z_H^{(L)}) \leq I\left(\mathcal{D}_s; \{Z_H^{(l)}\}_{l \in S_H} \cup \{Z_A^{(l)}\}_{l \in S_A}\right). \quad (27)$$

To decompose the above term, we introduce the following history sets:

$$\begin{aligned} H_A^{(l)} &= \{Z_H^{(l_1)}, Z_A^{(l_2)} \mid l_1 < l, l_2 < l, l_1 \in S_H, l_2 \in S_A\}, \\ H_H^{(l)} &= \{Z_H^{(l_1)}, Z_A^{(l_2)} \mid l_1 \leq l, l_2 < l, l_1 \in S_H, l_2 \in S_A\}. \end{aligned}$$

Applying the Chain Rule for Mutual Information [42], the above term is expanded as:

$$I(\mathcal{D}_s; \{Z_H^{(l)}\}_{l \in S_H} \cup \{Z_A^{(l)}\}_{l \in S_A}) = \sum_{l \in S_A} I(\mathcal{D}_s; Z_A^{(l)} | H_A^{(l)}) + \sum_{l \in S_H} I(\mathcal{D}_s; Z_H^{(l)} | H_H^{(l)}). \quad (28)$$

For each term  $l \in S_A$ , by the Chain Rule for Mutual Information, and considering the Markovian property of  $(A, Z_X^{(l)}) \rightarrow Z_A^{(l)}$ , we have:

$$\begin{aligned} I(\mathcal{D}_s; Z_A^{(l)} | H_A^{(l)}) &\leq I(\mathcal{D}_s, A, Z_X^{(l)}; Z_A^{(l)} | H_A^{(l)}) \\ &= I(A, Z_X^{(l)}; Z_A^{(l)} | H_A^{(l)}) + I(\mathcal{D}_s; Z_A^{(l)} | A, Z_X^{(l)}, H_A^{(l)}) \\ &\leq I(Z_A^{(l)}; A, Z_X^{(l)}). \end{aligned} \quad (29)$$

Similarly, for  $l \in S_H$ , given the Markovian property of  $(Z_A^{(l)}, Z_X^{(l)}) \rightarrow Z_H^{(l)}$ , we obtain the following inequality:

$$I(\mathcal{D}_s; Z_H^{(l)} | H_H^{(l)}) \leq I(Z_H^{(l)}; Z_A^{(l)}, Z_X^{(l)}). \quad (30)$$

To provide a computationally tractable objective, we introduce a variational approximation to the marginal distribution  $p(y)$ . Note that the mutual information can be expressed as:

$$I(X; Y) = \mathbb{E}_{p(x,y)} \left[ \log \frac{p(y|x)}{p(y)} \right].$$

Given an arbitrary variational distribution  $q(y)$ , we have:

$$\mathbb{E}_{p(x,y)} \left[ \log \frac{p(y|x)}{q(y)} \right] - I(X; Y) = \text{KL}(p(y) \| q(y)) \geq 0,$$

which leads to the variational upper bound:

$$I(X; Y) \leq \mathbb{E}_{p(x,y)} \left[ \log \frac{p(y|x)}{q(y)} \right]. \quad (31)$$

By applying this property to each term in the summation and substituting the definitions from Eq. 8, we arrive at the final inequality:

$$I(\mathcal{D}_s; Z_H^{(L)}) \leq \sum_{l \in S_A} \text{AIB}^{(l)} + \sum_{l \in S_H} \text{HIB}^{(l)}, \quad (32)$$

which concludes the proof.  $\square$

## B Computational Complexity

We analyze the complexity of the instantiated MLGIB under an efficient implementation based on sparse message passing and stochastic neighborhood sampling. Let  $n$  and  $m$  denote the numbers of nodes and edges, respectively; let  $l$  be the number of propagation layers; let  $h$  be the hidden dimensionality; let  $C$  be the number of labels; let  $d$  be the label embedding dimensionality; and let  $N_b$  and  $E_b$  denote the numbers of sampled nodes and edges in a mini-batch subgraph.

For full-graph training, the dominant cost of one MLGIB layer consists of three parts: (i) label-aware neighbor scoring in AIB, which requires  $O(nCd + mC)$  operations to construct label-aware node representations and compute edge-wise relevance scores; (ii) hierarchical information bottleneck modeling in HIB, which incurs  $O(mh^2)$  time for messages computation; and (iii) standard message aggregation and node update, which can be implemented in  $O(mh + nh^2)$  or  $O(mh^2)$ . Assuming  $m > n$ , we use an efficient implementation with a complexity of  $O(mh + nh^2)$ . Therefore, the overall time complexity of a  $l$ -layer MLGIB is  $O(l(nCd + mC + mh^2 + nh^2))$ . In sparse graphs, this can be viewed as near-linear in the number of edges up to moderate feature- and label-dependent factors. In practice, MLGIB is trained with stochastic neighborhood sampling rather than full-graph propagation. Under this setting, the per-mini-batch complexity becomes

$$O(l(N_bCd + E_bC + E_bh^2 + N_bh^2)), \quad (33)$$

which scales with the sampled subgraph size instead of the entire graph. This significantly improves practicality on large-scale graphs and makes the method compatible with standard mini-batch GNN training pipelines.

The space complexity mainly includes node representations  $O(nh)$ , pseudo-label embeddings  $O(nC)$ , and message embeddings  $O(mh)$ . Full-graph storage requires  $O(nh + mh + nC)$  memory, while the mini-batch version only stores sampled node/edge states, yielding

$$O(N_bh + E_bh + N_bC). \quad (34)$$

Overall, MLGIB preserves the sparse-computation advantages of modern GNN frameworks, while introducing only structured overheads associated with label-aware filtering and information-theoretic message compression. This design leads to a scalable implementation suitable for both medium- and large-scale multi-label graph learning.

## C Experiment Setup Supplement

### C.1 Dataset Supplement

To evaluate the effectiveness of the proposed framework, we conduct experiments on four real-world multi-label datasets that exhibit diverse characteristics:

- **DBLP** [34] depicts the co-authorship relation between authors. Each node represents an author, and each edge represents the existence of a co-authorship relation between two authors. The dataset comprises four distinct labels, each corresponding to a specific research domain. The feature vector for each author (node) is constructed by concatenating the textual content of the titles from all publications authored by the individual.
- **BlogCatalog** [35] is a prevalent benchmark in blogosphere analysis and network representation learning. In this network, nodes correspond to individual bloggers on the BlogCatalog platform. An edge is established between two nodes to represent a mutual friendship between the corresponding bloggers. Node labels are derived from the thematic categories of the blogs published by each user. Notably, this dataset does not provide intrinsic node attributes. To evaluate the efficacy of our proposed methodology and established baselines on node classification tasks within attribute-deficient networks, we employ randomly initialized node embeddings for the experimental validation.
- **PCG** [36] is employed for protein phenotype prediction. It consists of a network containing 3,233 nodes (proteins) and 37,351 edges. Each node is represented by a 32-dimensional feature vector. The multi-label classification task involves assigning nodes to one or more of 15 phenotype categories, where a phenotype denotes an observable characteristic associated with a disease. Edges in the graph represent functional interactions between protein pairs. The correspondence linking proteins to their associated phenotypes is curated from an open-source database.
- **Delve** [23] constitutes a large-scale citation network comprising 1,229,280 nodes (academic papers) and 4,322,275 edges. Within this graph, an edge is established from one node to another to represent a citation relationship between the corresponding publications. The classification task involves assigning each paper a subset of 20 predefined research field categories (indexed from 1 to 20), which serve as node labels.

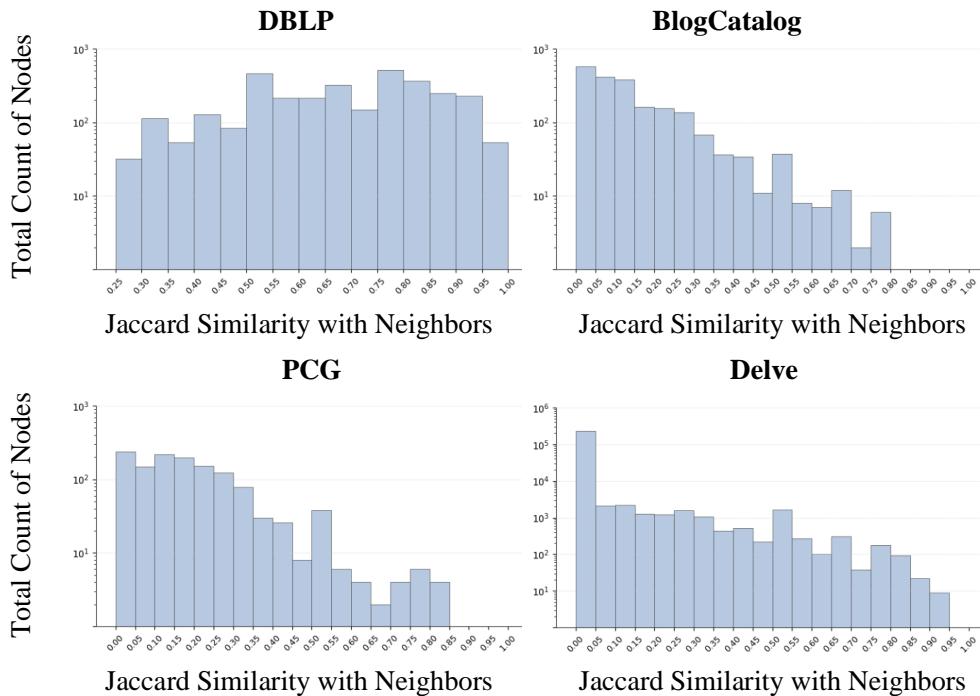


Figure 7: Distributions of label correlation among nodes.

A summary of the dataset statistics is reported in Table 3. We also analyze the distributions of label correlation among nodes, as shown in Fig. 7. Except for DBLP, most nodes in the other datasets exhibit low label similarity with their neighbors, which also validates the characteristic of partial label overlap for nodes in multi-label graphs that we proposed in Fig. 1(a).

Table 3: Dataset Statistics

Dataset	Nodes	Features	Classes	Edges
DBLP	28,702	300	4	68,335
BlogCatalog	10,312	300	39	333,983
PCG	3,233	32	15	37,351
Delve	1,229,280	300	20	4,322,275

**PubMed dataset (single-label) [39] in expressiveness analysis.** PubMed dataset is the standard node classification benchmark used in graph neural networks (GNNs). It models the citation network of biomedical literature. In this dataset, nodes represent scientific publications, and edges represent citation links. The dataset contains 19,717 nodes and 44,338 edges.

DBLP and BlogCatalog datasets are available at: <https://github.com/Tianqi-py/MLGNC>; PCG and Delve datasets are available at: <https://github.com/YuanchenBei/CorGCN>; The PubMed dataset is available via the `torch_geometric` function in PyTorch. These sources are not official releases. We randomly split the data into 60% for training, 20% for validation, and 20% for testing. All results are averaged over 10 independent runs with different random seeds.

## C.2 Metric Supplement

Following prior work on multi-label graph models [24, 22, 15], to comprehensively evaluate the performance of our multi-label graph model, we employed a suite of seven established metrics: Macro-AUC, Micro-AUC, Ranking Loss, Hamming Loss, Macro-AP, Micro-AP, and LRAP.

- Macro-AUC calculates the Area Under the Receiver Operating Characteristic Curve for each label independently and then averages the results, providing a class-aware measure that treats all labels equally. It is sensitive to the performance on minority labels.
- Micro-AUC computes the AUC by globally aggregating all predictions and true labels across all instances and labels, effectively treating the evaluation as a single binary classification task. It is more influenced by the performance on majority labels.
- Ranking Loss measures the average fraction of reversely ordered label pairs, where an irrelevant label is incorrectly ranked above a relevant one. It assesses the quality of the predictive ranking.
- Hamming Loss quantifies the fraction of misclassified instance-label pairs (i.e., wrong labels) to the total number of labels. It is a straightforward measure of overall classification error.
- Macro-AP computes the average precision (area under the precision-recall curve) for each label and then takes the arithmetic mean over all labels, offering a label-centric perspective on precision-recall trade-off.
- Micro-AP calculates the average precision from a globally aggregated contingency table of all predictions and true labels, providing an instance-centric perspective on overall precision and recall.
- LRAP (Label Ranking Average Precision) evaluates the quality of the ranked label list for each instance. For a given instance, it calculates the average precision over the set of its relevant labels, based on their ranks within the predicted ordering, and then averages this value across all instances. It directly measures how well the ranking surface relevant labels at the top.

### C.3 Compute Resources

All experiments were conducted on a server running Ubuntu 22.04 LTS, equipped with an Intel Core i9-10920X CPU (3.50 GHz base, 4.80 GHz max turbo frequency, 12 cores / 24 threads), 125 GB of system memory, and an NVIDIA RTX A6000 50GB GPU. The software environment included Python 3.9.18, PyTorch 2.4.0, and CUDA 12.4.

### C.4 Training Configuration

Our training process implements a graph information bottleneck-inspired approach for multi-label node classification. The configuration details are as follows:

- **Optimizer:** Adam with a learning rate of  $1 \times 10^{-3}$ .
- **Neighborhood Sampling:** Stochastic neighbor sampling with a fixed fanout of 1,024 per node at each layer.
- **Regularization:** The loss is employed with a dataset-specific hyperparameter  $\beta \in [0, 10^{-3}]$ .
- **Gaussian Mixture kernels:** For the Gaussian mixture distribution defined in the HIB module, we fix the number of mixture kernels to  $m = 6$ .
- **Reproducibility:** Deterministic execution using fixed random seeds and CUBLAS\_WORKSPACE\_CONFIG set to `:4096:8`.
- **Initialization:** Model parameters are initialized using Xavier uniform initialization to maintain stable gradient flow.
- **Mini-batch Training:** To handle the scale of the De1ve dataset, we employ stochastic neighbor sampling with a fixed fanout of 1,024 for each target node per layer.
- **Embedding Dimension:** The dimension of the label embedding space is set to  $d = 128$ .
- **Skip-gram Negative Sampling:** The positive-to-negative sample ratio is 1:5.
- **Skip-gram Batch Configuration:** To ensure efficient gradient updates on large-scale datasets like De1ve, we utilize a batch size of 1,024 for the label pairs.

## D Related Works and Discussion

In this section, we review the most related works, discussing the differences and connections between our work and existing methods.

### D.1 Multi-Label Graph Learning

As previously discussed, only a few studies have focused on Multi-Label Graph Learning. Representatively, ML-GCN [24] employs a skip-gram training strategy to learn the three-way relations between labels and labels, as well as between labels and nodes. Through joint optimization, it jointly derives the embeddings for both labels and nodes. This provides inspiration for the weight assignment of messages in our theoretical instantiation. LANC [22] incorporates a label-attention mechanism at the final layer, which inserts a label vector correlated with the features. This vector comprises a combination of the label information most relevant to the features, and is used to predict the final labels. Similar to the idea of assigning message-passing weights according to label relevance in this study, LARN [23] proposes a Label-Guided Neighbor Aggregator Module to aggregate node neighbors with different weights. Going further, CorGCN [15] learns separate graphs for the number of labels in order to disentangle ambiguous features and structure. Information propagation and aggregation are performed on each graph, and the results are then merged for final prediction.

**Discussion.** Although the aforementioned methods leverage attention mechanisms or multi-label correlations to achieve a certain degree of effectiveness, they lack a principled information-theoretic foundation. Consequently, they fail to filter and purify multi-label message propagation, and thus remain limited by the multi-label over-squashing problem caused by the compression of diverse label information. Our proposed MLGIB method introduces the information bottleneck principle into multi-label graph message passing, filtering and purifying the information flow, thereby alleviating multi-label over-squashing by filtering noisy information during propagation.

### D.2 Over-Squashing in Multi-Label Graphs

As previously discussed, the over-squashing issue becomes prominent when GNNs attempt to convolve or aggregate information from long-range nodes in a graph [6]. As the number of GNN layers increases to reach distant nodes, information from an exponentially growing receptive field is forced to be compressed into fixed-length node embeddings. Thus, conventional GNNs struggle to effectively propagate messages from distant nodes and tend to overemphasize local information.

From a Riemannian geometry perspective, over-squashing has been attributed to negatively curved edges in the graph [7]. To address this issue, the Stochastic Discrete Ricci Flow (SDRF) algorithm modifies the graph structure by adding or removing edges around negatively curved regions. Similarly, BORF [26] further establishes the connection between over-squashing and graph geometry, proposing a spatial graph rewiring strategy to alleviate this phenomenon. More recently, this line of research has linked over-squashing to graph curvature and spectral gaps, motivating the development of spectral rewiring methods such as FOSR [25], which introduces a computationally efficient approach to mitigate over-squashing by directly optimizing the spectral gap of the input graph.

**Discussion.** MLGIB differs from existing literature in three aspects. (1) **Multi-Label Awareness.** Existing over-squashing alleviation methods are primarily designed for single-label graphs and do not consider that over-squashing is aggravated by the crowding of multiple label signals in multi-label graphs. In contrast, MLGIB mitigates the over-squashing problem on multi-label graphs by assigning label-relevant information to nodes. (2) **Information Preservation.** Curvature- and rewiring-based approaches alleviate over-squashing by modifying the input graph structure to reduce topological bottlenecks. However, such modifications may disrupt the original relational semantics of nodes, potentially leading to information loss in multi-label graphs. Because local homogeneity is diminished in multi-label graphs, altering the graph topology tends to inject additional irrelevant label information—essentially noise. (3) **Targeted and Task-Adaptive Design.** Graph rewiring methods typically optimize structural properties such as curvature or spectral gaps in a task-agnostic manner. In contrast, MLGIB is formulated as an end-to-end framework. All instantiated components are designed to serve the objective function, giving the model a high degree of task-driven focus, which in turn delivers higher performance for downstream multi-label node-classification tasks.

## **E Limitations**

The core idea of MLGIB is to filter out label information irrelevant to the target node via the information bottleneck. Its effectiveness relies, to some extent, on the learnable label co-occurrence patterns (i.e., label correlations) present in the graph. If the labels of a node and its neighbors are almost random and exhibit very weak correlation (i.e., the “homophily” is extremely low), the model may struggle to learn effective message-passing paths ( $Z_A^{(L)}$ ) and relevant messages ( $Z_H^{(L)}$ ), potentially limiting performance gains.

## **F Broader Impact**

Although our work is primarily fundamental, focusing on enhancing the capabilities of GNNs to process graph-structured data, the improvements introduced by MLGIB can also significantly benefit various downstream tasks. These applications include a wide range of graph-related tasks, such as optimizing information flow in social networks, enhancing pattern recognition in fraud networks, and improving performance on other complex graph-based analyses.